6(2009) 385 – 412

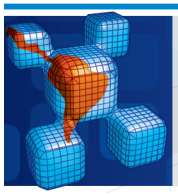

Latin American Journal of Solids and Structures
www.lajss.org

Energy absorption characteristics of annealed steel tubes of various cross sections in static and dynamic loading

Abstract

Thin walled structures are used as energy absorbing elements in various applications. These elements, when axially loaded, fold progressively which make them as good energy absorbing elements. The circular tube proves to be a popular energy absorber because it provides a reasonably constant operating force which is the primary characteristics of the energy absorber. Square and rectangular tubes are widely used in automobile structures as these cross sections are suitable for welding with other components in the structure and hence highly preferred. In the present study annealed steel tubes of the above three shapes are made for the same cross - sectional area and are subjected to axial compression to find out the efficiency of these tubular sections. The energy absorbing characteristics of these cross sections are studied under static and dynamic loading conditions. The effect of impact velocity is studied by keeping the striking mass constant and varying the drop height. The experimental results are compared with the available analytical models and good agreement is found.

Keywords

specific energy absorption, thin walled sections, annealed tubes, dynamic loading.

R. Velmurugan[a,*] **and R. Muralikannan**[b]

[a]Dept. of Aerospace Engg IIT Madras, Chennai - 36 – India
[b]Dept. of Mechanical Engg IIT Madras, Chennai - 36 – India

Received 15 Jun 2009;
In revised form 25 Oct 2009

* Author email: ramanv@iitm.ac.in

1 INTRODUCTION

Thin walled tubes represent the most widely used collapsible impact energy absorbers, owing to their high frequency of occurrence as structural elements. The most common shapes are circular, square and rectangular. These tubes are used as front and side impact beams in automobiles. For these applications, the energy absorption characteristics of these tubes are to be evaluated to quantify the energy absorbed by the tubes of different cross sections. The progressive collapse of circular tubes may occur in two modes, one in symmetrical convolution called concertina or axisymmetric mode of collapse, the other one in diamond mode of collapse in which both transverse and longitudinal folding are formed. Square and rectangle tubes exhibit symmetric, asymmetric mixed mode and extensional collapse mode under static and

NOMENCLATURE

R	mean radius of the circular tube
D	diameter of the circular tube
A	cross sectional area of the tubes
B	side of the square tube
c, d	sides of rectangular tube
C	$C = (c + d)/2$
h	wall thickness of the tube
L	length of the tube
M_o	perfectly plastic bending moment of tube wall per unit length
H	half wavelength of fold
L_e	effective crushing length
P_m	static mean load
P_k	static peak load
P_m^d	dynamic mean load
P_k^d	dynamic peak load
σ_o	flow stress
σ_y	yield stress
ψ	static energy absorbing effectiveness factor
ψ'	dynamic energy absorbing effectiveness factor
G	mass of the striker
ε_r	rupture strain
δ_r	final axial displacement
V	impact velocity
σ_y^d	dynamic yield stress
σ_u	ultimate tensile strength
K, ρ	Cowper- Symonds equation constant
$\dot{\varepsilon}$	strain rate
v	final velocity
u	initial impact speed
a	acceleration
t	time

dynamic loading. Opposite lobes deforming in a similar manner, all the four lobes deforming inwards and three lobes deforming inwards and one lobe deforming outwards are categorized as symmetric mode of collapse. In asymmetric mixed mode A, three lobes deform outwards and one lobe deforms inwards. In asymmetric mixed mode B two adjacent lobes deform inwards and the other two adjacent lobes deform outwards [2].

Alexander [10] proposed a simple analytical model for the study of axisymmetric fold pattern. In this model the external work done was equated with internal work from bending at three stationary plastic hinge locations in the tube and circumferential stretching of the

metal between the hinges. Pugsley and Macaulay [12] considered the asymmetric fold and developed the empirical models. Johnson et al. [1] attempted to develop a theory for the non-symmetric mode based on the actual geometry of folding, with the tube material at the mid-surface being considered inextensional. Hence they were able to develop equations to predict average axial crush force, FAV. However, the agreement between the model and the test results for P.V.C. tubes was not encouraging.

Wierzbicki and Abramowicz [11] studied the axial crushing of rectangular tubes. In their study it was found that two third of plastic energy was dissipated through inextensional deformation at stationary and moving plastic hinges. Abramowicz and Jones [1] conducted axial compression tests on a range of thin walled circular and square tubes. They analyzed the different types of crushing modes developed in circular and square tubes. Effective crushing length term was introduced in their analytical model. Singace et al [4] developed a new model for the axisymmetric collapse of circular tubes. In their model they considered both the inward and outward radial displacement of the tube. The geometry is governed by a geometric eccentricity factor m, which is defined as the ratio of outward fold length to total fold length.

Gupta and Velmurugan [3] determined the folding parameter experimentally. They observed that the fold formation was not symmetric about its mid-plane and the extent of internal folding in each tube was dependent on its D/t ratio. It was also observed that the folding length increased with the increase in folding parameter from 0 to 0.5 and thereafter it decreased which implied that fold length was maximum when internal and external fold were equal. Guillow et. al [9] conducted quasi static axial compression tests on thin walled circular aluminium tubes and found that the ratio of peak load to mean load increased substantially with the increase in D/t ratio. Langseth and Hooperstad [5] carried out experimental investigation to study the behaviour of square thin walled aluminium extrusions in static and dynamic loading. The experimental results showed that the dynamic mean load was significantly higher than static mean load for the same displacement. G.C. Jacob *et al* [6] study the energy absorption of polymer composite materials. In their work, they emphasize the importance of controlled energy absorption and energy absorption rate. N. Jones [8] introduced the energy absorbing effectiveness factor in his study. This dimensionless factor compares the effectiveness of the energy absorber for different shape and materials.

The present work is to study the energy absorption characteristics of steel tubes in annealed condition for different shapes when subjected to static and dynamic loading. The ductility of the tubes is increased by annealing the tubes at 9100 C and cool it in air. It is observed that the energy absorption depends on the plastic deformation of tubes. The increase in ductility of the material increases the plastic flow which will result in uniform operating force. The uniform operating force is one of the desirable characteristics of the energy absorber. In this work, tubes of three different cross sections are subjected to axial compression. The effect of shape in mean load and specific energy absorption of the tubes is studied. The effect of impact velocity in energy absorption characteristics of different cross sections is also studied by keeping the striking mass constant and varying the drop height. Static tests are carried out in a 200 kN UTM and the dynamic tests are conducted in Instrumented Drop Mass setup.

2 MATERIAL PROPERTIES

The circular tube, made up of mild steel with diameter of 75 and thickness of 1.6 mm is the parent tube. The rectangular and square tubes are fabricated by drawing from the circular tubes. All the three tubes have the same cross sectional area. The square tubes have the side of 60 mm and the rectangular tubes are of 70mm x 50mm size. Annealing of the specimens is done by slow cooling through ferrite-pearlite field. The micro structure of the annealed specimens at 500 x magnification is shown in the Fig. 1. It clearly shows the ferrite structure (white) and pearlite structure (dark).

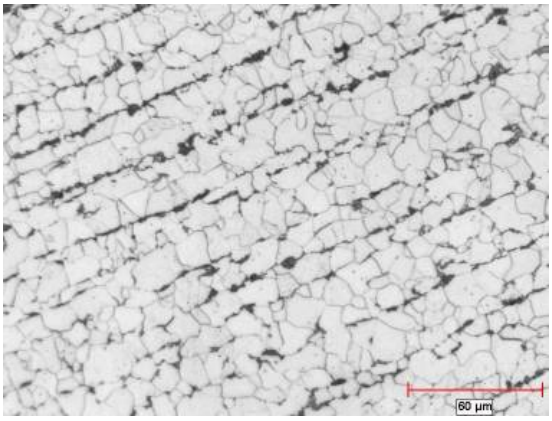

Figure 1 Microstructure of annealed specimen.

To determine the mechanical properties of the material, tensile test specimens were cut from the tubes as per the ASTM E-04 standards. The test specimens were taken from the sidewalls which are parallel to the extrusion direction. Specimens were subjected to axial compression in the UTM of 20 tonne capacity. Yield strength and ultimate tensile strength of the specimens are found out from the stress strain curve and the results are given in Table 1. It is observed that the yield strength of the circular specimens is less than square and rectangular tubes. Fig. 2 shows typical stress-strain curves for the test specimens. The curves show the ductile nature of the specimens.

Table 1 Mechanical properties of the test specimens.

S.No	Specimen geometry	Specimen size (mm)	Yield strength (MPa)	Ultimate tensile strength (MPa)
1	Circular	75 x1.6	266.94	398.63
2	Square	60x60x1.6	314.12	441.56
3	Rectangular	70x50x1.6	292.99	399.74

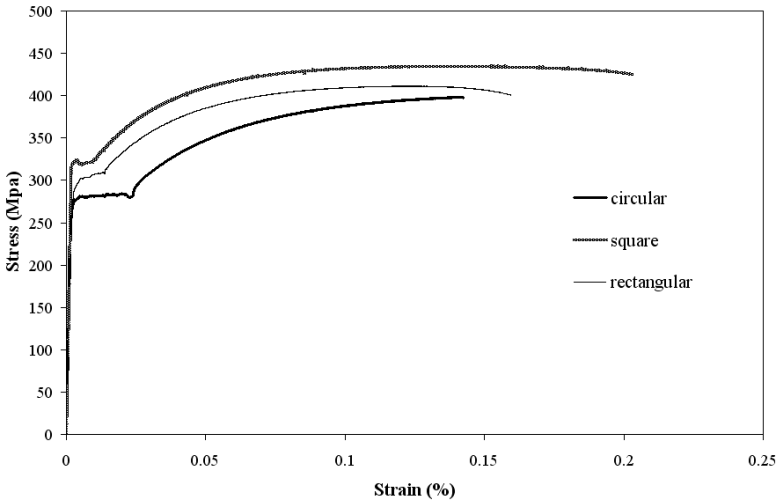

Figure 2 Tensile test results of the specimens.

3 QUASI STATIC TEST

Prior to testing, the wall thickness of the specimens is measured and the variation in thickness relative to the average value was less than 5%. Tubes are subjected to axial compression in the UTM. The thickness of all the tubes is 1.6 mm. Aspect ratio of 2 is maintained for all the cross sections. The dimensions and mass of each specimen are measured. The average length of the circular specimen is 150 mm and the mass is 0.447 kg. The average length of square tube is 120 mm and for rectangular tube it is 140 mm and the corresponding mass values are 0.355 kg and 0.412 kg, respectively.

3.1 Circular tubes

The results of the quasi static axial compression tests are given in Table 2. The tested circular tube specimens are shown in Figure 3(a). The circular tubes exhibit mixed mode in static compression. The folding process starts with axi-symmetric mode and then shifted to diamond mode. The outward fold length is higher than inward fold length. The average wave length of first fold is 19.5 mm. The wavelength of subsequent folds is increased up to 24 mm. After the formation of diamond mode there is no revert back to axi-symmetric mode. The load displacement curves obtained are shown in Fig 4. The load deflection curve shows clear peaks and valleys which are directly related to the number of folds in the specimen. The load value increases up to a maximum value and drops after the formation of plastic hinges. Again the load value increases which are corresponding to the formation of second fold but the second peak value is less than the first peak. From the load displacement curves obtained from the experiments, the energy absorbed by the tubes is calculated. The specific energy absorption is obtained by calculating the energy absorbed per unit crushing mass. Abramowicz and Jones [1] provided expression for the average crushing force of circular tubes for concertina mode of failure as

$$P_m = 86.14 M_o \left(\frac{2R}{h}\right)^{1/3} \tag{1}$$

where

$$M_o = \left(\frac{2\sigma_o}{\sqrt{3}}\right)\left(\frac{h^2}{4}\right) \tag{2}$$

Table 2 Quasi static test results of tubes of different cross sections.

Specimen	Crush length (mm)	Energy absorbed (J)	Peak load (kN)	Mean load (kN)	Specific Energy Absorption (kJ/kg)
Circular	70.3	3716.4	106.5	52.86	17.50
Circular	71.6	3916.1	106.6	54.69	18.18
Circular	72.9	3925.2	104.1	53.84	18.06
Square	80.0	2894.3	99.3	36.17	12.26
Square	67.8	2650.1	110.1	39.08	13.28
Square	86.5	3428.9	109.1	39.64	13.00
Rectangular	80.0	2702.8	109.5	33.78	11.43
Rectangular	96.8	3472.5	115.6	35.87	12.38
Rectangular	79.8	2952.5	97.9	36.99	12.58

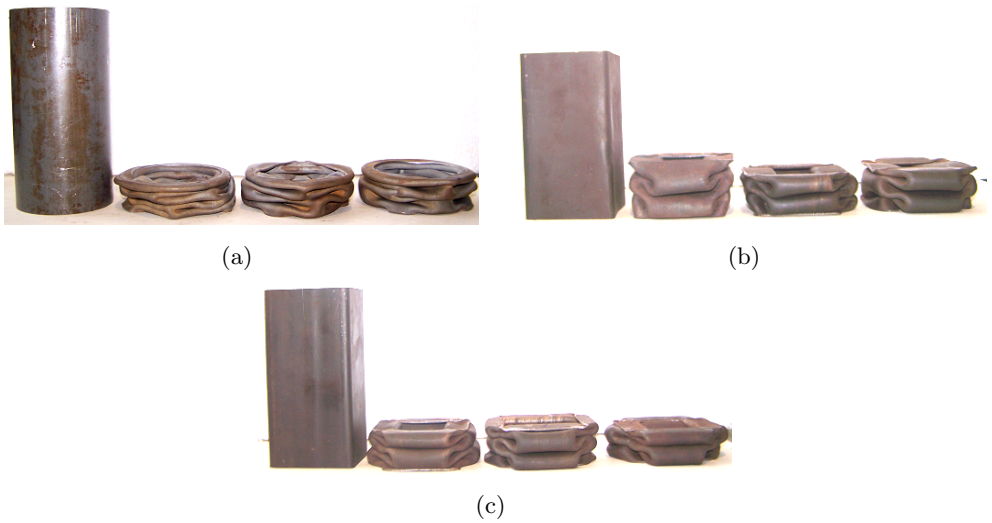

(a) (b)

(c)

Figure 3 Quasi static compression test. (a) Circular tubes, (b) Square tubes and (c) Rectangular tubes.

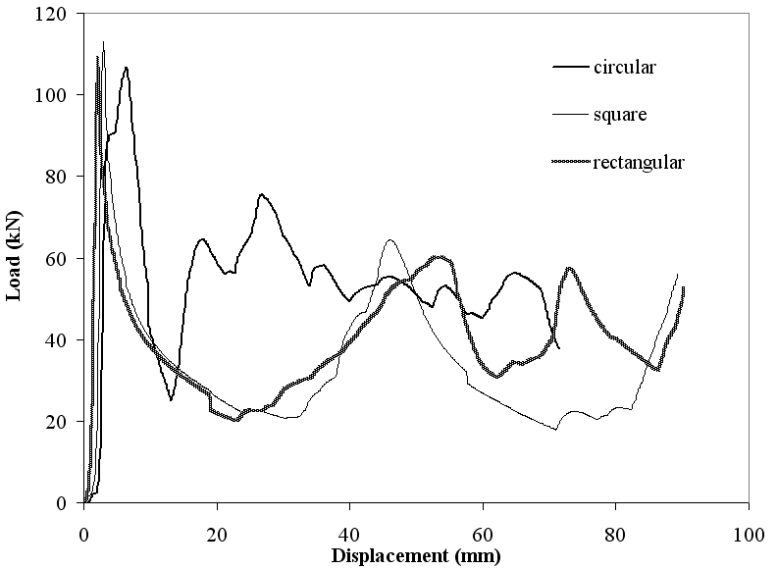

Figure 4 Load displacement curves of the quasi-static tests.

The mean load is calculated theoretically by using the above expression. The theoretical results show good agreement with the experimental results. The mean load of circular tubes in static compression is in the range of 54 kN. The specific energy absorption for the above tube is around 18 kJ/kg. The ratio of peak load to mean load value is 2.

3.2 Square tubes

The square tubes exhibit symmetric crush mode in static compression. The compressed specimens are shown in Figure 3(b). As the load is applied two faces fold inward and the opposite two faces fold outwards. The length of the subsequent folds is higher than the first fold. The inward movement of side walls increases the subsequent fold length and the inward portion is subjected to lateral crushing. The average wave length of first fold is 40 mm and for the subsequent folds it is around 46 mm. The distance between the plastic hinges in square tube is higher than the circular tube by virtue of its shape. The load deflection curve also shows that the wavelength of square tube is higher than circular tube. The expression to find the mean load for the square tubes [1] is

$$P_m = 52.22 M_o \left(\frac{B}{h}\right)^{1/3} \tag{3}$$

Where M_o is the perfect plastic bending moment capacity which is given by

$$M_o = \sigma_o \left(\frac{h^2}{4}\right) \tag{4}$$

The load is calculated by using the expression and shows good agreement with the exper-

imental results. The mean load for square tubes in static compression is around 39 kN and the corresponding specific energy absorption is around 13 kJ/kg. The peak load to mean load ratio is 2.75.

3.3 Rectangular tubes

The rectangular tubes are also subjected to axial compression and the deformed specimens are shown in Figure 3(c). The rectangular tubes undergo symmetric, asymmetric A and B and extensional crush mode in static compression. The symmetric mode of collapse is observed in static compression tests. In all the specimens two opposite faces fold inwards and other two faces fold outwards. It is observed that the minor side folds outwards and major side folds inwards. The wavelength of fold is around 40 mm. The mean load for rectangular tubes in static compression is around 36 kN. The specific energy absorption for square tubes is around 13 kJ/kg. The peak load to mean load ratio is about 3.25. It is observed that the specific energy absorption of rectangular and square tubes is less than circular tubes. This is attributed to the variation of wavelength in the three shapes. In rectangular and square tubes the fold length is higher than that in circular tubes and hence the mean load for square and rectangular tubes is less than that of circular tubes. That is the arm length between two hinges of rectangular and square tubes are higher than the circular tubes. The wavelength of fold increases the length of the tube crushed without absorbing the energy. The effective crushing distance given by the expression [1]

$$\left(\frac{L_e}{2H}\right) = 0.77 \tag{5}$$

The fold length of circular tubes is less than the rectangular and square tubes which means that the circular tubes more efficiently utilized than the square and rectangular tubes. So by keeping the circumferential area and material properties constant, we observe that the specific energy absorption capacity of circular tube is high by virtue of its shape. The average crushing force for the rectangular tubes [12] is

$$P_m = 38.27 M_o \left(\frac{C}{h}\right)^{1/3} \tag{6}$$

The effective crushing distance is not included in this expression. When the effective crushing distance is included the theoretical prediction has good agreement with the experimental results. The peak load to mean load ratio of circular tubes is less than the rectangular and square tubes.

4 DYNAMIC TESTS

Impact experiments are conducted by Instrumented Drop Mass setup which is shown in Fig 6. The drop mass system has the flexibility to vary the impact mass and drop height, by which we can provide various input energy value to the specimens. The striking mass is an assembly

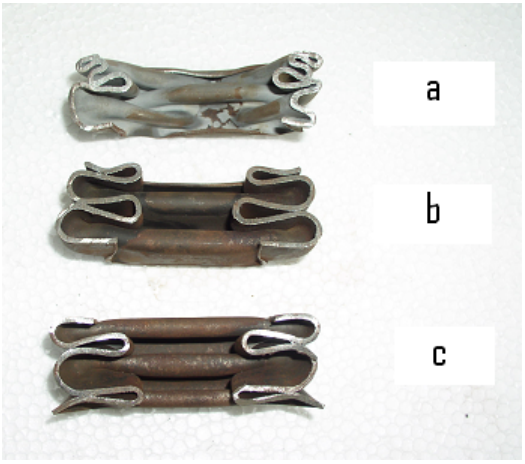

Figure 5 Cut section view of the quasi static test specimens: (a) circular tubes, (b) square tubes and (c) rectangular tubes.

of circular discs of 7 kg and 10 kg mass. Depending on the energy requirement we can add the discs to the assembly so the striking mass can be varied from 10 to 150 kg. The assembly is lifted by an electro magnet through the guide pipe. After reaching the desired height the electromagnet is de-magnetized and the striking mass is dropped and falls freely through the guide pipe. The guide pipe ensures the directions of the striking mass. The maximum velocity achieved by this setup is 10 m/s. The velocity of the striking mass just before the impact is measured using the laser – photo diode setup. Two photo diodes are kept in parallel and separated by a known distance of 80 mm and these diodes sense the laser light. When the striking mass cuts the first beam the counter starts and when it cuts the second beam the counter stops. The velocity of the striking mass is calculated using the time taken by the mass to cross the known distance. The load time history of the striking mass is recorded by using a high sensitivie load cell. The data is captured by National Instruments, Data Acquisition System and the data is analyzed through Labview software. The accelerometer is fixed on the striking mass and the signal is acquitted through NI data acquisition system. The signals are twice integrated with respect to time to get the actual displacement. The load time history and displacement time history are cross plotted to get the load displacement curve. From the load displacement curves, the work done is calculated. A low pass filter is used to filter the noise signals. The drop mass used is 103 kg. Experiments are performed for the impact velocities of 7.0, 7.7 and 8.3 m/s. The tubes are placed over the platen without any support. The load cells are kept under the platen.

4.1 Circular tubes

The circular tubes exhibit three types of crushing modes in dynamic tests. Axi-symmetric, diamond and mixed mode are found in specimens as the velocity is increased. The deformed specimens are shown in Fig. 7. Depending on the impact velocity the crushing modes are

Figure 6 Instrumented drop mass setup.

changing. Axi-symmetric mode is found in the 7m/s velocity range and mixed mode is found in the velocity range of more than 7.7m/s. The load displacement curves for different impact velocities are given in Fig 8. The first peak load which causes the first fold is clearly seen in the figure and subsequent peaks are also visible. The first fold absorbs certain amount of impact energy and rest of the energy creates subsequent folds. The first peak value increases with the increase in impact velocity. Unlike static compression there is no distinct relation between peaks in the load deflection curve and the number of folds in the specimen. Similar observations are also made in dynamic crushing of thin walled aluminium extrusions earlier [9]. The mean load and specific energy absorption are obtained from the experiments are given in Table 3. The mean load and specific energy absorption increases with increase in impact velocity. The peak load to mean load ratio is around 2.25. The mean load for dynamic loading [12] is given by the expression

$$P_m^d = P_m \left(1 + \left(\frac{\dot{\varepsilon}}{K}\right)^{1/\rho}\right) \tag{7}$$

where

$$\dot{\varepsilon} = 0.37\left(\frac{V}{R}\right) \tag{8}$$

Here $\dot{\varepsilon}$ is the strain rate, K and ρ are constants. For mild steel the values of K is 6844 s^{-1} and ρ is 3.91. The experimental results are compared with the analytical model for three different stress values corresponding to lower yield point, proof stress and upper yield point. The experimental values show good agreement with the analytical value when the proof stress values are used for the impact velocity of 8.3 m/s. The comparisons are shown in Fig. 9.

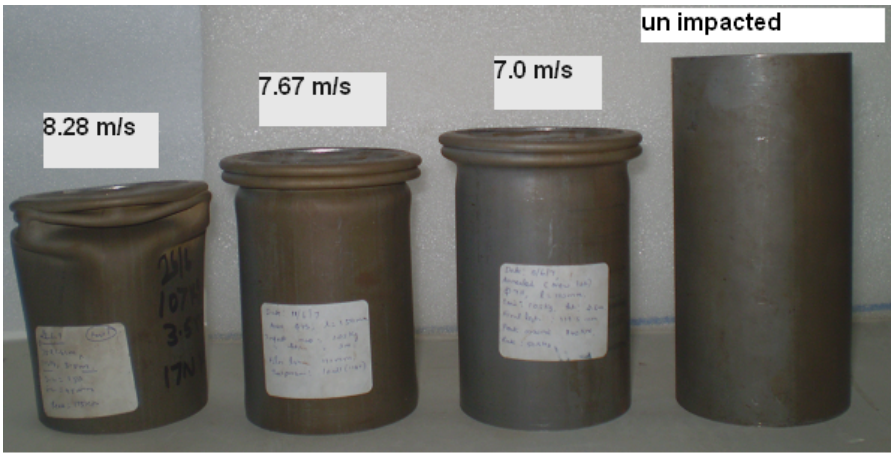

Figure 7 Circular specimens impacted at different velocities.

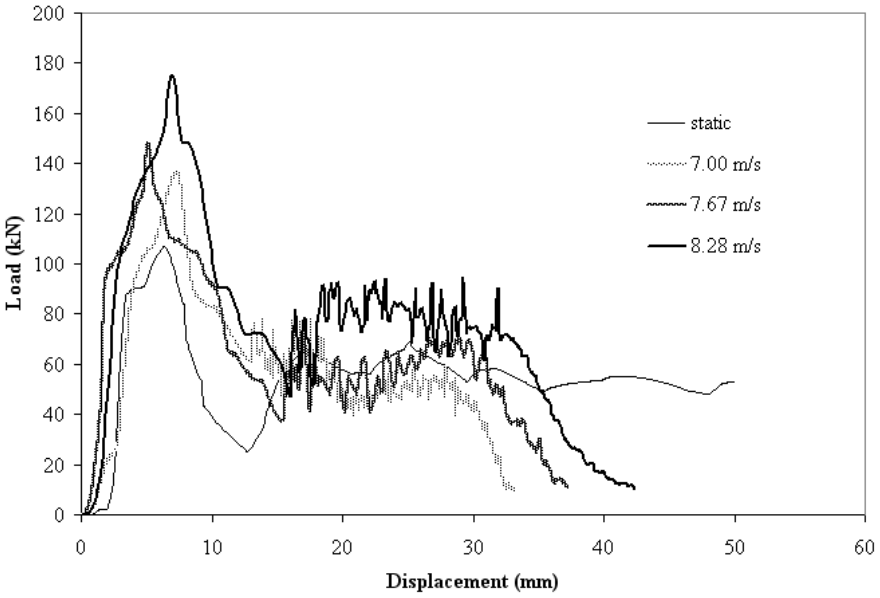

Figure 8 Load displacement curves of the circular tubes impacted at different velocities.

Table 3 Dynamic test results of diameter 75 mm, 1.6 mm circular tubes.

Impact velocity (ms^{-1})	Crush distance (mm)	Peak load (kN)	Work done (kJ)	Mean load (kN)	Specific energy absorption (kJ/kg)
7.00	33.1	135.42	1950.30	58.92	19.77
7.00	33.8	132.50	2048.20	60.60	20.33
7.00	31.7	140.00	1902.10	60.00	20.14
7.7	36.5	141.50	2238.30	61.32	20.58
7.7	37.2	147.35	2395.30	64.39	21.61
7.7	34.8	146.20	2264.80	65.08	21.84
8.3	39.2	152.30	2652.20	67.66	22.70
8.3	42.4	175.24	3028.30	71.42	23.97
8.3	45.1	169.80	3193.20	70.80	23.76

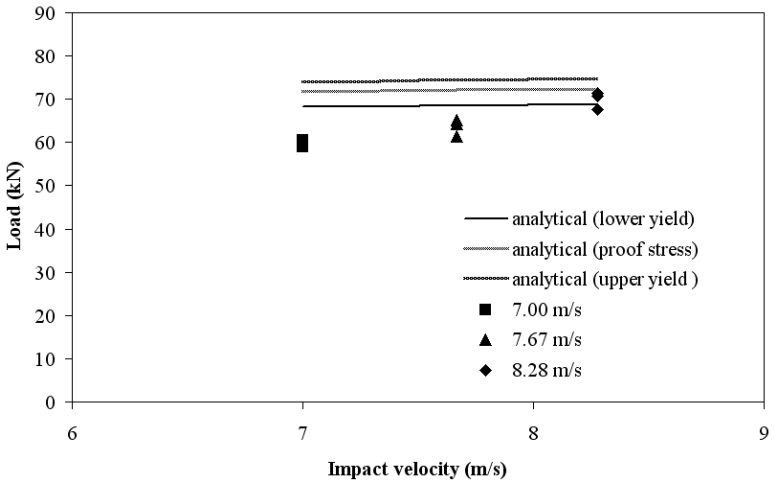

Figure 9 Comparison of experimental results with analytical model for circular tubes.

4.2 Square tubes

Square tubes are subjected to impact loading and the tested specimens are shown in Figure 10. Symmetric mode of collapse is observed for the velocity range of 6.26 m/s and 7.28 m/s. The peak load in symmetric mode of collapse is less than other modes. In one kind of symmetric mode, two opposite faces fold inward and other two faces fold outward and absorbs less energy than the other symmetric mode, where three faces fold inward and one face fold outward. Asymmetric mode of collapse B is observed for the impact velocity of 8.3 m/s. Two adjacent lobes of the tube deform inwards and two adjacent lobes deform outwards. The load displacement curve for different impact velocities are given in Figure 11. The first peak load which causes the first fold is clearly seen in figure and subsequent peaks also visible. The first fold absorbs certain amount of impact energy and rest of the energy creates subsequent folds.

Figure 9 shows that one complete fold is formed for the velocity of 7.0 m/s and two complete folds are formed for the velocity of 8.3 m/s. The mean load and specific energy absorption are increasing with the increase of impact velocity and these values are less than the mean load corresponding to circular tubes. The expression to find the strain rate effect in symmetric mode of deformation for square and rectangular tubes [1] is given by

$$\dot{\varepsilon} = 0.33\left(\frac{V}{c}\right) \tag{9}$$

The values obtained from the expression are used in Eq. (7) to get the mean load.

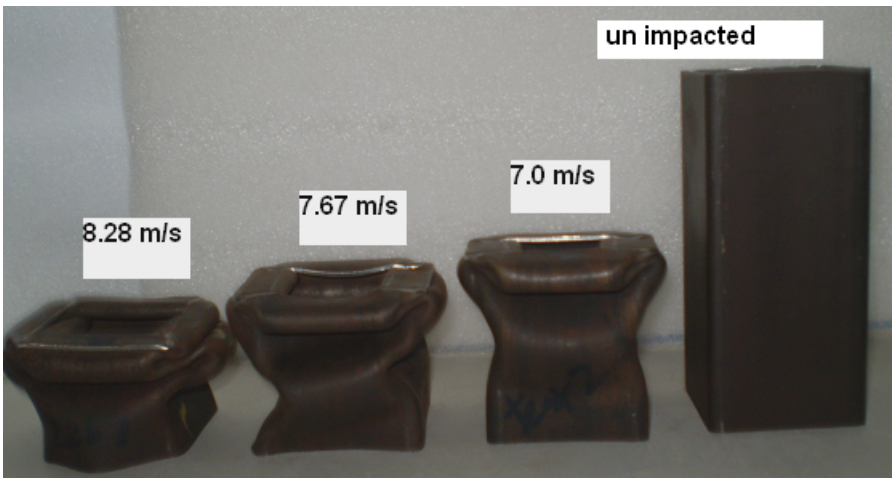

Figure 10 Square specimens impacted at different velocities.

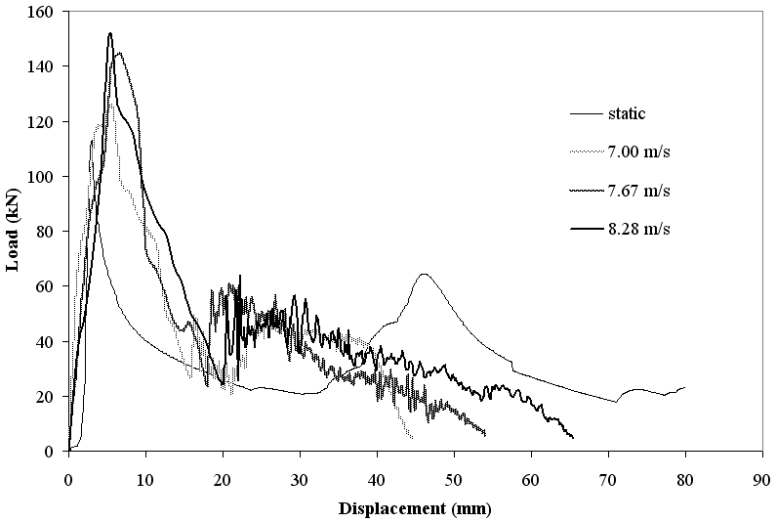

Figure 11 Load displacement curves of the square tubes impacted at different velocities.

The experimental mean load values are compared with the analytical results and are given in Fig. 12. The experimental results are in good agreement with the analytical value when the strength value corresponding to the upper yield point is used for the impact velocities 7.7 m/s and 8.3 m/s. The peak load to mean load ratio is around 3 for all the velocities.

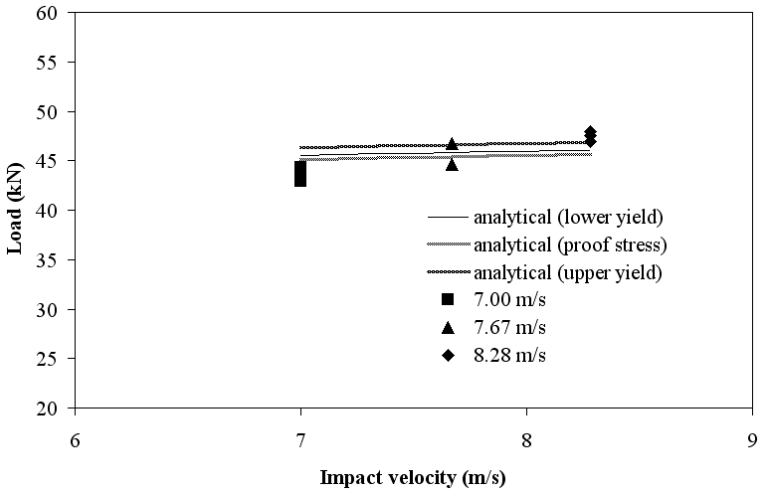

Figure 12 Comparison of experimental results with analytical model for square tubes.

Table 4 Dynamic test results of square 60x60 mm and thickness 1.6mm tubes.

Impact velocity (ms^{-1})	Crush distance (mm)	Peak load (kN)	Workdone (kJ)	Mean load (kN)	Specific energy absorption (kJ/kg)
7.00	44.5	125.07	1923.4	43.22	14.61
7.00	47.2	114.10	2023.3	42.87	14.49
7.00	46.1	117.20	2045	44.36	14.99
7.7	52.4	132.40	2448.5	46.73	15.80
7.7	51.8	143.90	2310.5	44.60	15.08
7.7	54.0	144.41	2522.6	46.71	15.79
8.3	65.5	151.76	3140.2	47.94	16.21
8.3	63.8	155.00	2991.5	46.89	15.85
8.3	64.2	146.70	3054.3	47.57	16.08

4.3 Rectangular tubes

Rectangular tubes exhibit different types of collapse modes in impact loading unlike in quasi static loading. The impacted rectangular specimens are shown in Fig. 13. The mean load, Peak load and specific energy absorption are calculated and the results of the tests are given in Table 5. The initial peak load increases with the increase in impact velocity. It is also

observed that the peak load is sensitive to geometrical imperfections of the tubes and hence there is a difference in peak value, for the same impact velocity. The load displacement curves for different impact velocities are given in Figure 14. It is observed that the initial peak values are higher than the corresponding quasi static value. The ratio between the dynamic peak value to static peak value is more than 3 in rectangular tubes. For the impact velocity of 8.3 m/s, it is around 3.75. The mean value is calculated by using the expression (7) and (9) and it is observed that the experimental results are in good agreement with the analytical values when the proof strength values are used in Eq. (7). The comparisons are given in Fig. 15.

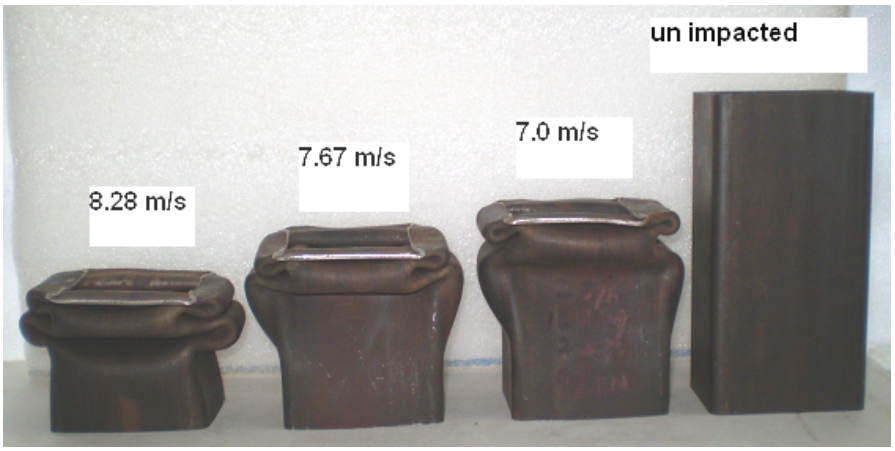

Figure 13 Rectangular specimens impacted at different velocities.

Table 5 Dynamic test results of rectangular 70x50 mm and thickness 1.6 mm tubes

Impact velocity (ms^{-1})	Crush distance (mm)	Peak load (kN)	Workdone (kJ)	Mean load (kN)	Specific energy absorbtion (kJ/kg)
7.00	46.1	119.78	1793.8	38.91	13.22
7.00	50.4	112.00	2051.5	40.70	13.83
7.00	52.4	120.90	1956.1	37.33	12.69
7.7	60.5	140.70	2478.3	40.96	13.92
7.7	58.6	131.68	2361.5	40.30	13.69
7.7	58.2	128.50	2402.5	41.28	14.03
8.3	69.8	161.80	2918.4	41.81	14.21
8.3	71.4	162.78	3082	43.17	14.67
8.3	68.5	148.40	2875.2	41.97	14.26

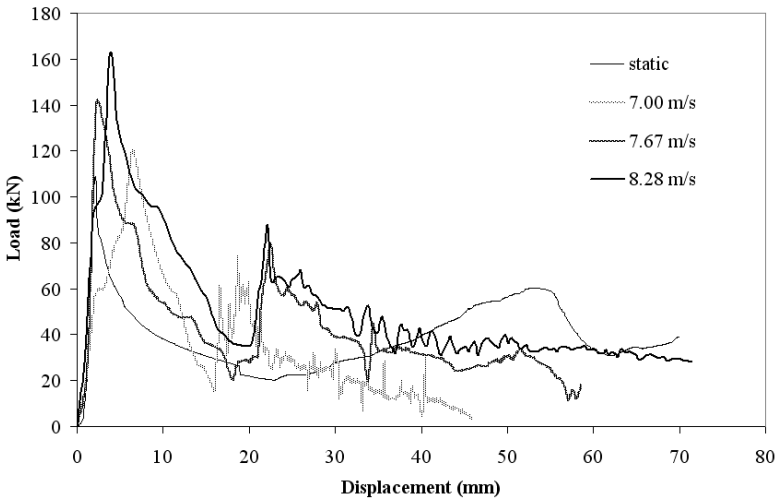

Figure 14 Load displacement curves of the rectangular tubes impacted at different velocities.

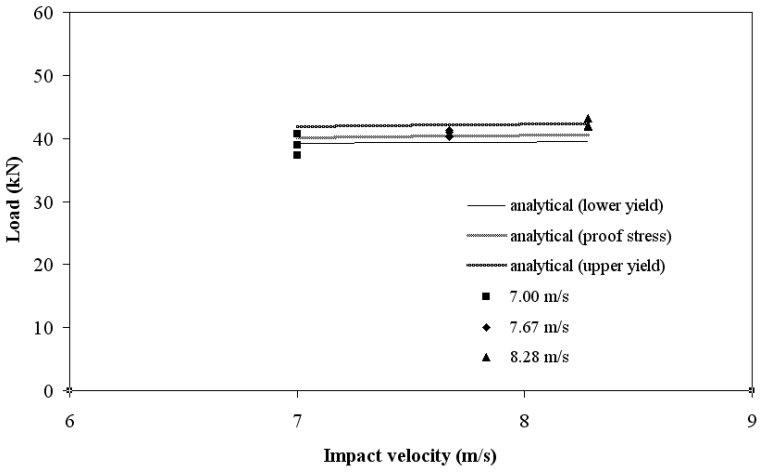

Figure 15 Comparisons of experimental results with analytical model for rectangular tubes.

5 COMPARISONS OF STATIC AND DYNAMIC STUDIES

From the experimental results, it is observed that the mean load corresponding to the dynamic loading is higher than static loading, which is observed in all the sections. The mean load for dynamic loading is 10% higher than the static loading for velocity of 7 m/s and it is 20% higher for 8.3 m/s. From the load displacement curves of the tubes, it is observed that the energy required to create the first fold in dynamic loading is higher than that required in static loading. For the impact velocity of 7.00 m/s there is no significant difference in mean load after the initial peak portion. The results are shown in Figs. 8, 11 and 14. For the impact velocity of 8.3 m/s the mean load after the initial peak is significantly higher than the static case. In static test the circular tubes mostly fold in mixed mode and some times in concertina

mode. But in dynamic loading the circular tubes folds in concertina mode for 7.0 m/s velocity range and in mixed mode for the velocity range of 8.3 m/sec. In static loading of the square and rectangular tubes, the opposite faces fold in the same direction. But in impact loading the specimens fold differently. In square tubes three faces of the tube fold inwards and one-face folds outwards. In rectangular tubes the opposite faces fold in opposite directions. The initial peak load and deformation mode are dependent on the friction effects, geometric and material imperfections. So there are variations in initial peak load of the tubes tested for the same velocity.

The increase in peak load is associated with inertia effects in impact due to the lateral movement of sidewalls in order to initiate the folding process. For low velocity, the first peak is in the region of static test, so there is not much difference in the specific energy absorption. The other factor account for the increase in energy absorption is the strain rate sensitivity of the material. Due to strain hardening the yield stress increases in impact loading and the expression is given by [1]

$$\sigma_o^d = \sigma_o \left(1 + \left(\frac{\dot{\varepsilon}}{K}\right)^{1/\rho}\right) \tag{10}$$

The mean load of crushing is dependent on the yield strength of the material. The yield strength of the material increases with the increase in impact velocity. So the energy required to make subsequent folds is higher in specimens subjected to impact loading than those in static loading. The analytical results match the mean load well, for higher velocities in square and rectangular tubes, when the strength corresponding to upper yield point is used for analysis.

6 STUDY OF ENERGY ABSORPTION RATE

The energy absorption rate of the circular tubes is given in Table 6. The rate for the initial fold is less than 1521 kJ/s and for subsequent folds the value is less than 100 kJ/s. The energy absorption rates of the square and rectangular tubes are given in Tables 7 and 8 respectively. From these tables it is seen that the initial fold the value is less than 1521 kJ/s for the impact velocities up to 7.7 m/s. The value is increased further when the impact velocity is increased to 8.3 m/s. The energy absorption rates of subsequent folds are less than 130 kJ/s. The load increases very rapidly in the initial stages of crushing to a maximum value beyond that stable crushing takes place. Current legislation for automobiles requires that vehicles should be designed such that, in the event of impact at speeds up to 15.5 m/s with a solid, immovable object, the occupants of the passenger compartment should not experience a resulting force that produces a net deceleration greater than 20g. The kinetic energy of the car of mass 1000 kg traveling at a velocity of 15.5 m/s is equal to 120.1 kJ. In the event of impact, the crashworthy materials should absorb this kinetic energy over a time frame that ensures the deceleration of the car to be less than 20g [6], above which the passengers will experience irreversible brain damage because of the relative movements of the various part of the brain i.e with in skull cavity. So, 120 kJ of work needs to be done on the crashworthy material. Hence

a material used for crashworthiness study has to be studied for impact energy of 120 kJ. The minimum time over which this work needs to be done, to ensure the safety of the passengers, is obtained using the basic equation of motion.

$$v = u - at \tag{11}$$

Where v is the final velocity and is equal to zero since the car comes to rest after collision. u is the initial impact speed and a is the maximum allowable deceleration which is equal to 20g. For the initial velocity of 15.5 m/s, The minimum time calculated to be equal to 0.079s. So the allowable rate of work decay, which will ensure the safety of passengers, is equal to 1521 kJ/s [7]. The Figs. 24-26 clearly indicate that the energy absorption rate is high at the initial stages of impact and then decreases rapidly. In all the tests, the tubes subjected to impact are not equipped with triggering mechanism. This is the main reason for increased energy absorption rate in the initial stages. The triggering mechanisms like chamfering the end of the tube will reduce the energy absorption rate. Figs. 24-26 show the energy rate vs time curves for the tubes impacted for different velocities. From the curves it is evident that the increase in impact velocity does not increase the energy absorption rate considerably. So if we are using a proper triggering mechanism the energy absorption rate can be made well below the 1521 kJ/s mark for the impact velocity of 15.5 m/s.

Table 6 Energy absorption rate for circular tubes.

Impact velocity (m/s)	Time taken for initial fold (ms)	Energy absorbed (J)	Energy rate (kJ/s)	Time taken for subsequent fold (ms)	Energy absorbed (J)	Energy rate (kJ/s)
7.00	1.40	1435.00	1025.0	11.94	1313.70	110.02
7.00	1.55	1045.60	674.60	13.70	1011.90	73.86
7.7	1.65	1420.00	860.60	12.80	1107.40	86.51
8.3	1.20	1895.20	1579.33	12.50	1400.40	112.03
8.3	1.55	1420.00	916.73	16.45	1912.30	116.25
8.3	1.20	1405.60	1171.33	15.35	1930.10	125.74

7 PERFORMANCE EVALUATION OF TUBES FOR DIFFERENT CROSS SECTIONS

The load displacement curves of the three cross sections corresponding to different impact velocities are given in Figs. 16-18. The impact energy applied to the tubes is calculated based on the drop mass and the height. The energy absorbed by the tube is obtained from the load displacement curve. Fig. 19 shows the percentage of impact energy absorbed by the tubes corresponding to different impact velocities. The average energy absorption of the tubes is about 80% of the input impact energy. The remaining energy is converted in to heat energy during collision. Fig. 20 shows the mean load of the tubes of different cross sections when subjected to impact loading. From these curves it is seen that the mean load of circular tubes

Table 7 Energy absorption rate for square tubes.

Impact velocity (m/s)	Time taken for initial fold (ms)	Energy absorbed (J)	Energy rate (kJ/s)	Time taken for subsequent fold (ms)	Energy absorbed (J)	Energy rate (kJ/s)
7.00	1.40	1826.80	1304.85	14.75	1112.50	75.42
7.00	1.55	1988.90	1283.16	15.70	971.59	61.88
7.7	1.45	1499.10	1033.86	22.25	1128.90	50.73
7.7	1.45	1841.90	1270.70	21.75	1155.70	53.13
7.7	1.50	1409.60	939.73	21.35	1048.10	49.09
8.3	1.65	1223.40	741.45	21.85	1116.50	53.15
8.3	1.65	1715.10	1039.45	20.85	1471.10	70.55

Table 8 Energy absorption rate for rectangular tubes.

Impact velocity (m/s)	Time taken for initial fold (ms)	Energy absorbed (J)	Energy rate (kJ/s)	Time taken for subsequent fold (ms)	Energy absorbed (J)	Energy rate (kJ/s)
7.00	1.50	1514.80	1009.86	18.85	1022.30	54.23
7.7	1.15	1530.30	1330.95	21.05	970.16	46.08
7.7	1.30	1369.20	855.70	20.60	1535.70	74.54
8.3	1.15	2206.30	1918.52	25.40	1999.20	78.70
8.3	1.35	1766.40	1308.44	21.15	1843.70	87.17

is higher than the rectangular and square tubes. The mean load for circular tubes, is 40% higher than the square tube values and is 50% higher than the values of rectangular tubes. Among the square and rectangular tubes the mean load of square tubes is 12% higher than that of rectangular tubes. The specific energy absorption of the tube is obtained from the load displacement curves and it is observed that the specific energy absorption of circular tubes is higher than the values of square and rectangular tubes. The comparative study is shown in the Fig. 21. All the three cross sections absorb same amount of impact energy but the mean load and specific energy absorption is different for different cross sections. This difference is attributed to the effective crushing length factor. For the circular tubes, the fold length is shorter than square and rectangular. The average fold length for circular tube is about 19.5 mm but for the square and rectangular tubes it is 38.5mm and 40 mm respectively. So, for every fold, the undeformed tube length between the tube hinges is higher for square and rectangular tubes than the circular tube. This makes the circular tube more efficient than the other tubes. The peak load to mean load ratio for circular tubes is in the range of 2.2 to 2.4. Square tubes have this ratio is in the range of 2.6-3.3 and for rectangular tubes it is in the range of 2.7-3.7. The time taken to reach the first peak in the load displacement curve is one of the important factors in design of energy absorbing structures. This time taken to reach

the first peak decreases with the increase of impact velocity and it is also influenced by the shape of the tube. It is high in circular tubes than the square and rectangular tubes. This comparison is shown in Fig. 22. There is no significant difference in time taken by the load curve to reach the first peak in square and rectangular tubes. The time needed to complete the entire process of crushing circular tubes is less than rectangular and square tubes. The comparison of time curves to complete the crushing process is given in Fig. 23. The study is made for different impact velocities. Square tubes take less time than rectangular tubes.

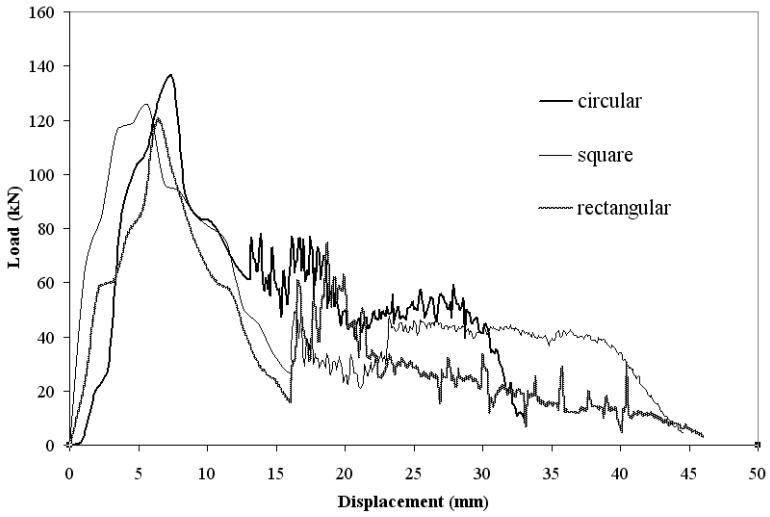

Figure 16 Comparison of load displacement curves of the three shapes for the impact velocity of 7.00 m/s.

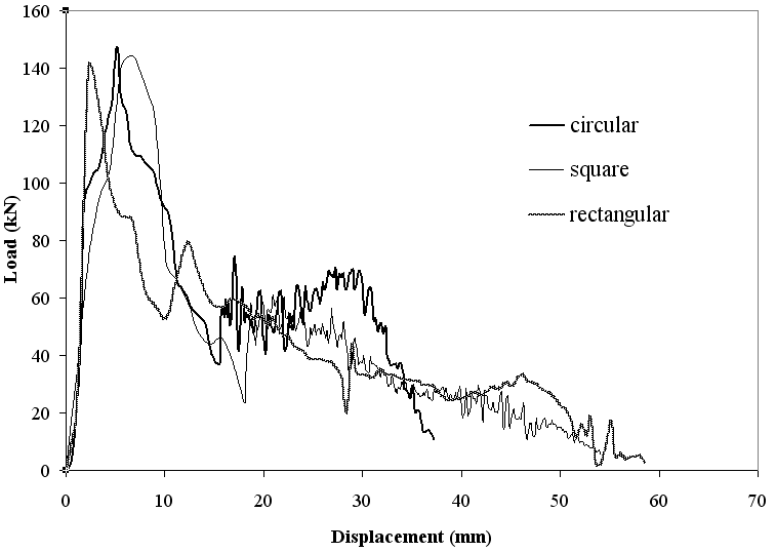

Figure 17 Comparison of load displacement curves of the three shapes for the impact velocity of 7.7 m/s.

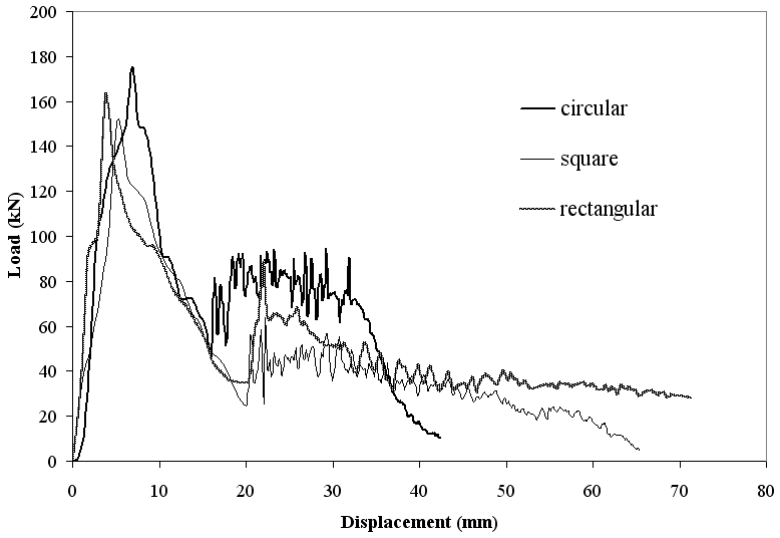

Figure 18 Comparison of load displacement curves of the three shapes for the impact velocity of 8.3 m/s.

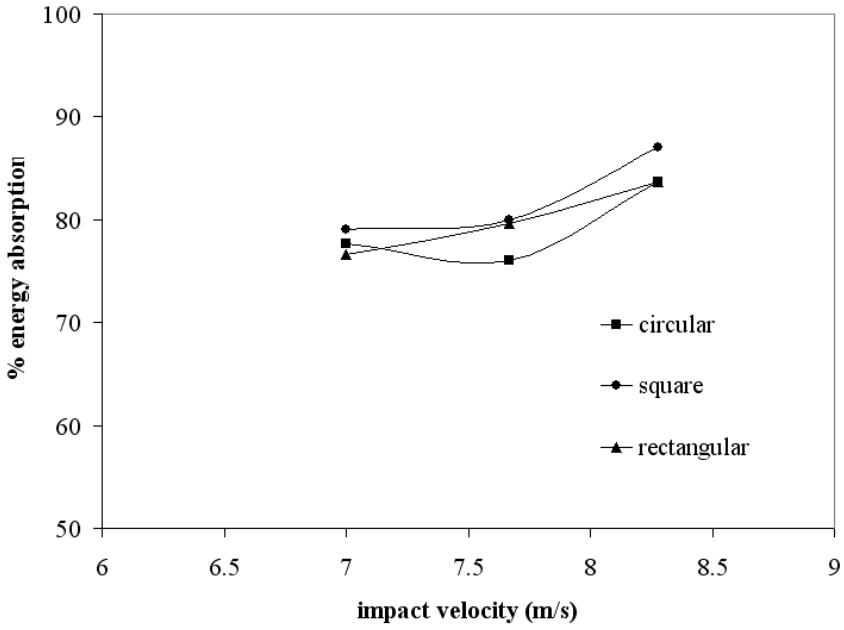

Figure 19 Comparison of % energy absorption between three cross sections in dynamic loading.

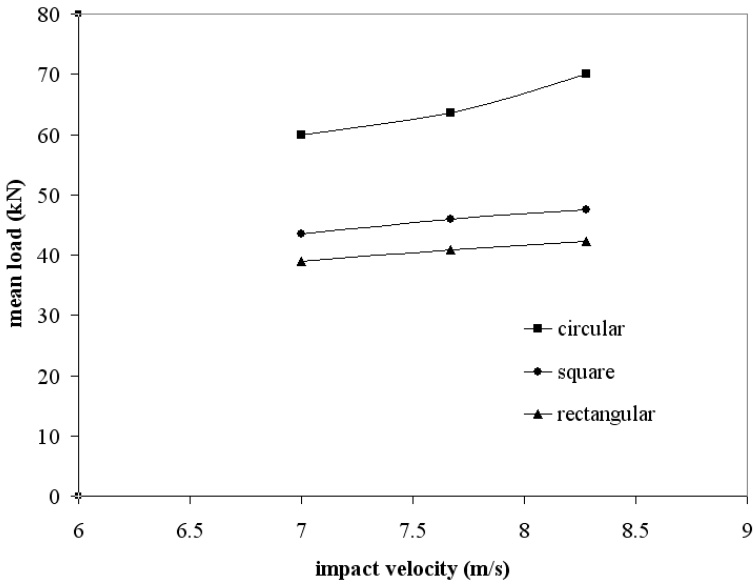

Figure 20 Comparison of mean load between three cross sections in dynamic loading.

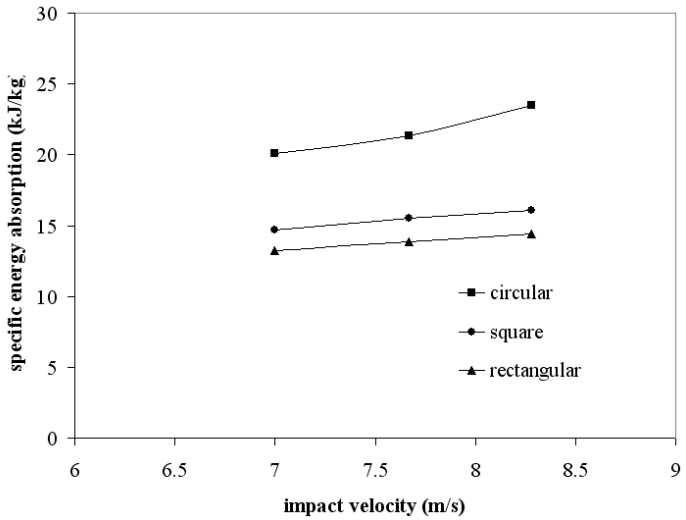

Figure 21 Comparison of specific energy absorption between three cross sections in dynamic loading.

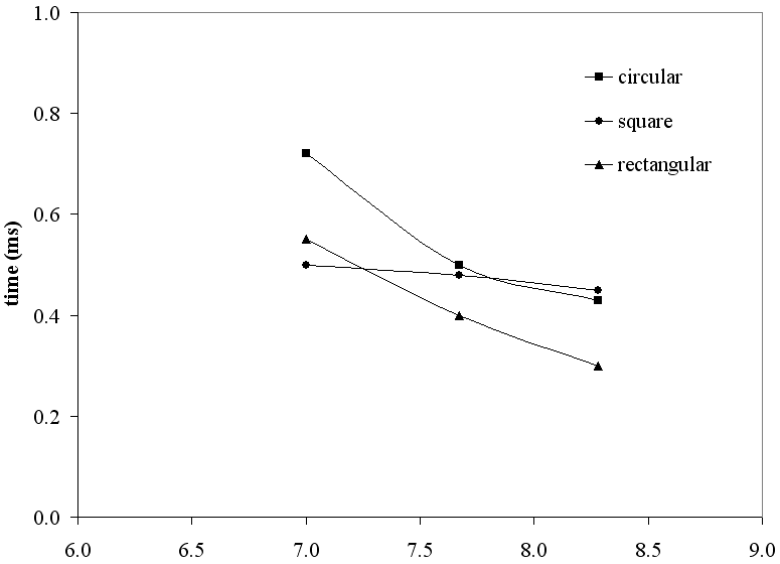

Figure 22 Comparison of time required to initiate the fold.

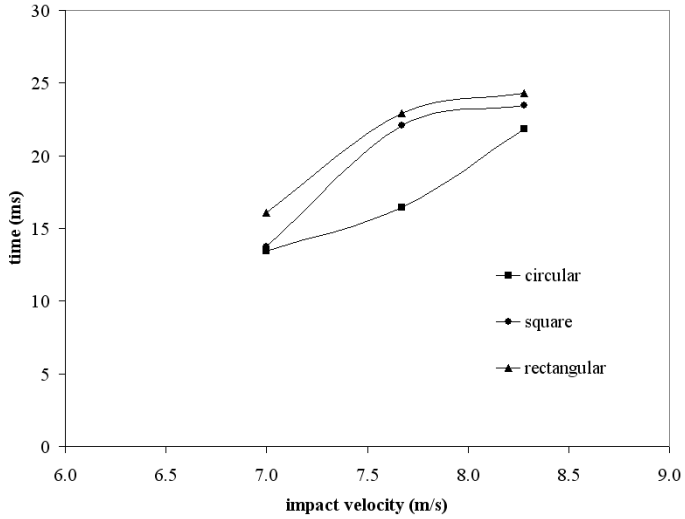

Figure 23 Comparison of time required to complete the folding process.

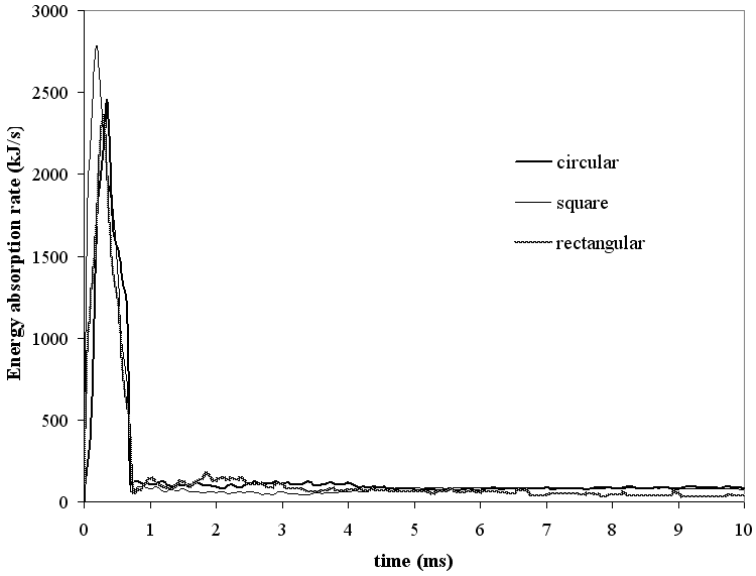

Figure 24 Comparison of energy absorption rate for the impact velocity of 7.00 m/s.

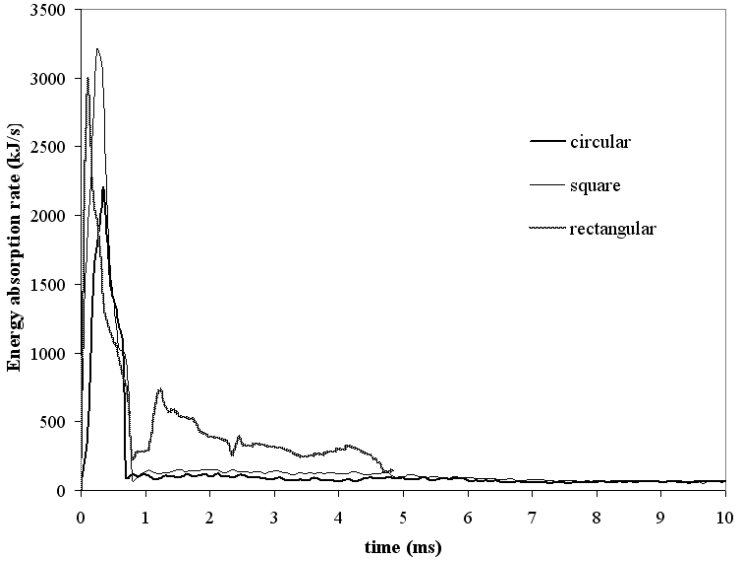

Figure 25 Comparison of energy absorption rate for the impact velocity of 7.7 m/s.

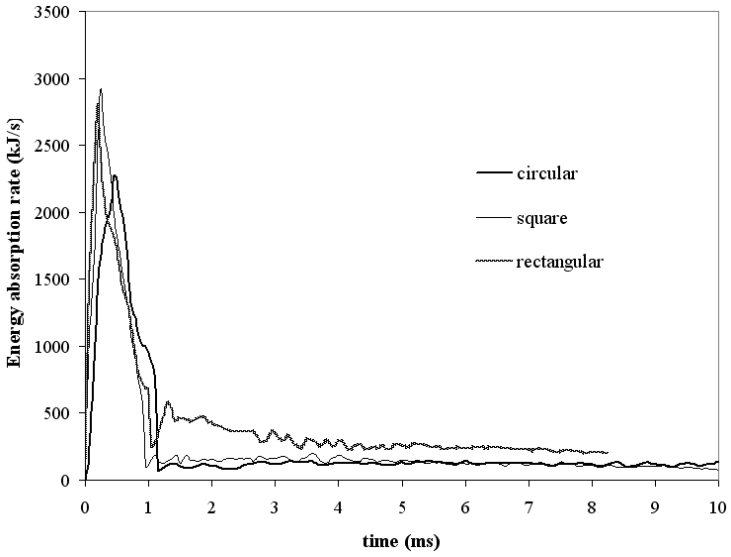

Figure 26 Comparison of energy absorption rate for the impact velocity of 8.3 m/s.

8 ENERGY ABSORBING EFFECTIVENESS FACTOR

The energy absorbing effectiveness factor is a dimensionless number used to indicate the effectiveness of the energy absorber. Using this factor we can compare the energy absorption of specimens made up of different materials and shapes. It is defined as the ratio between the total elastic and plastic strain energy absorbed by a structural member to the energy absorbed in the same volume of material up to failure in tension [8]. The expression for static axial compression is given by the Eqn.(12).

$$\psi = \frac{3P_m}{4A\sigma_o\varepsilon_r} \tag{12}$$

Where σo is the flow stress and εr is the rupture strain. For the impact loading it is given by the expression

$$\psi' = \frac{3GV_o^2}{8\sigma_o A\delta_f\varepsilon_r} \tag{13}$$

The energy effectiveness factor for static axial compression is given in Table 9. The study shows that the circular cross section is more effective than square and rectangular cross sections. The energy effectiveness factor is calculated for annealed and dual phase tubes, for all the three cross sections. It is observed that circular tubes are almost in the same range, when compared the annealed tube results with the dual phase tubes.

In impact tests also the circular tubes shows higher effectiveness than the other two cross sections. This is shown in the Fig. 27. When compared with the dual phase steel tubes, it is observed that the circular cross section of annealed tube is on par with the effectiveness of dual phase steel tubes. This is shown in Fig. 28. In case of square and rectangular tubes the

Table 9 Energy absorbing effectiveness factor for Annealed and dual phase steel tubes

Specimen	**Circular**	**Square**	**Rectangular**
Annealed	2.30	0.96	1.20
Dual phase	2.42	2.33	1.99

energy absorbing effectiveness factor of dual phase steel tube is higher than annealed tubes. This is shown in Figs. 29-30.

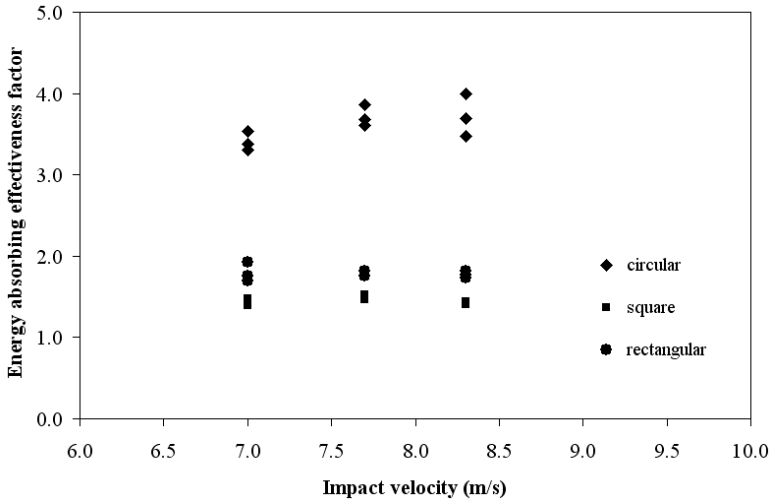

Figure 27 Comparison of energy absorbing effectiveness factor between three cross sections.

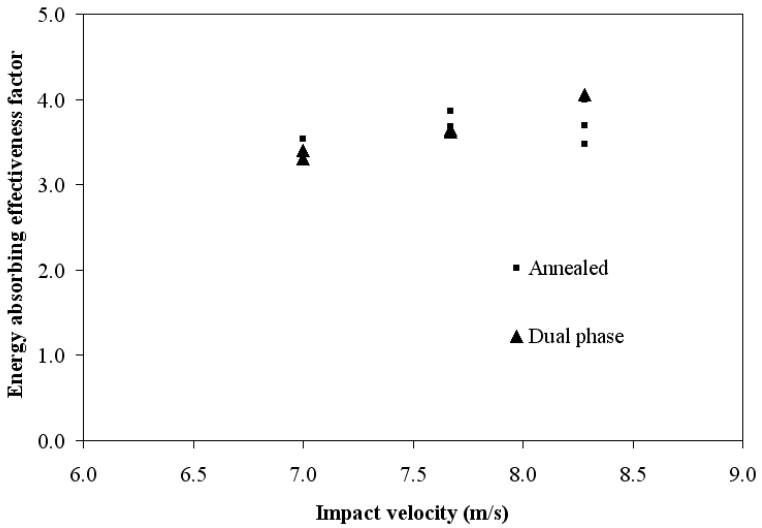

Figure 28 Comparison of energy absorbing effectiveness factor between annealed and dual phase circular steel tubes.

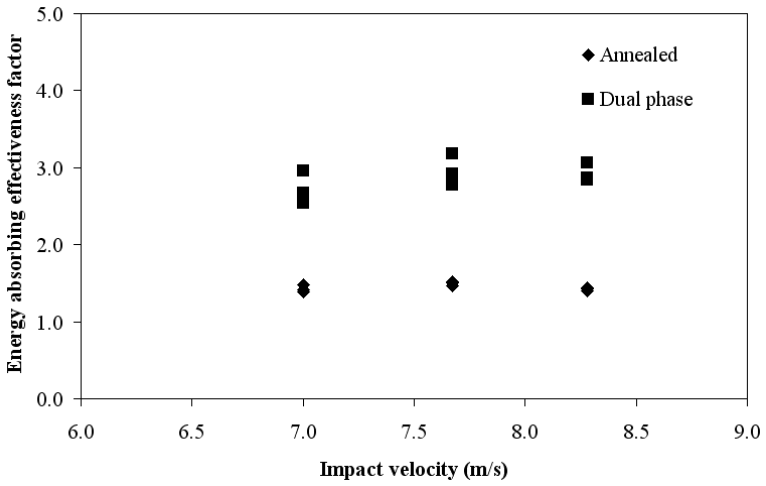

Figure 29 Comparison of energy absorbing effectiveness factor between annealed and dual phase square steel tubes.

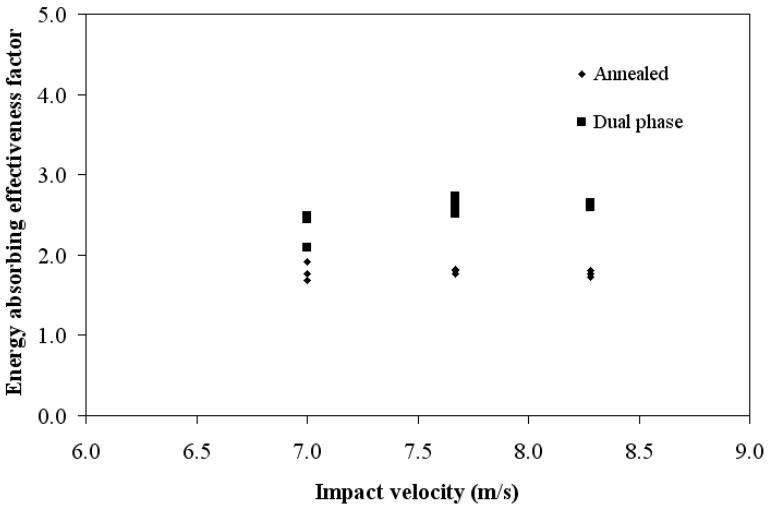

Figure 30 Comparison of energy absorbing effectiveness factor between annealed and dual phase rectangular steel tubes.

9 CONCLUSION

Static and dynamic tests were conducted for tubes of different cross sections, namely, circular, square and rectangular. From the results it is observed that tubes absorb more energy in impact loading than quasi-static condition. The tubes exhibit different types of collapse mode in impact when compared to quasi static. The study shows that the specific energy absorption for circular tube is higher than square and rectangular tubes. Among the square and rectangular tubes, the square tubes absorb more energy than rectangular tubes. The mean load in static

and dynamic studies has good agreement with the theoretical values. The ratio of peak load to mean load is also calculated and all the three types of tubes have same kind of the ratio but the peak load in circular tubes is higher than the square and rectangular tubes.

Acknowledgement This work is supported by Tubes Investments of India Ltd, Avadi, Chennai-54, India.

References

[1] W. Abramowicz and N. Jones. Dynamic progressive buckling of circular and square tubes. *Int. J. Impact Engng*, 4(4):243–270, 1986.

[2] J.M. Alexander. An approximate analysis of the collapse of thin cylindrical shells under axial loading. *Q J Mech Appl Maths*, 13:10–15, 1960.

[3] S.R. Guillow, G. Lu, and R.H. Grzebieta. Quasi static axial compression of thin-walled circular aluminium tubes. *International Journal of Mechanical Sciences*, 43:2103–2123, 2001.

[4] N.K. Gupta and R. Velmurugan. An analysis of axi-symmetric axial collapse of round tubes. *Thin walled structures*, 22:261–274, 1995.

[5] D. Hull. Energy absorbing composite structures. *Sci and Tech Rev, University of Wales*, 3:23–30, 1998.

[6] George C. Jacob, John F. Fellers, Srdan Simunovic, and Michael J. Starbuck. Energy absorption in polymer composites for automotive crashworthiness. *Journal of composite materials*, 36(7):813–849, 2001.

[7] W. Johnson, P.D. Soden, and S.T.S. Al-Hassani. Inextensional collapse of thin-walled tubes under axial compression. *Journal of Strain Analysis*, 12:317–330, 1977.

[8] N. Jones. Energy absorbing effectiveness factor. *International Journal of Impact Engineering*, 2009. doi: 10.1016/j.ijimpeng.2009.01.08.

[9] M. Langseth and O.S. Hopperstad. Static and dynamic axial crushing of square thin walled aluminium extrusions. *Int J of impact Engg*, 18(7-8):949–968, 1996.

[10] A. Pugsley and M. Macaulay. The large scale crumpling of thin cylindrical columns. *Quart. J. Mech. Appl.Maths*, 13:1–9, 1960.

[11] A.A. Singace, H. Elsobky, and T.Y. Reddy. On the eccentricity factor in the progressive crushing of tubes. *Int J of Solids and Structures*, 32(24):3589–3602, 1995.

[12] T. Wierzbicki and W. Abramowicz. On the crushing mechanics of thin walled structures. *Journal of applied mechanics*, 50:727–734, 1983.